Task Specific Robust Grasping For Multifingered Robot Hands

George I. Boutselis, Charalampos P. Bechlioulis, Minas V. Liarokapis and Kostas J. Kyriakopoulos

Abstract— **In this paper, we propose a complete methodology for deriving task-specific force closure grasps for multifingered robot hands under a wide range of uncertainties. Given a finite set of external disturbances representing the task to be executed, the concept of Q distance is introduced in a novel way to determine an efficient grasp with a task compatible hand posture (i.e., configuration and contact points). Our approach takes, also, into consideration the mechanical and geometric limitations imposed by the robotic hand design and the object to be grasped. In addition, incorporating our recent results on grasping [1], the ability of the robot hand to exert the required contact forces is maximized and robustness against positioning inaccuracies and object uncertainties is established. Finally, the efficiency of our approach is verified through an experimental study on the 15 DoF DLR/HIT II robotic hand attached at the end effector of the 7 DoF Mitsubishi PA10 robotic manipulator.**

I. Introduction

Every day life experience and recent neuroscientific studies on human grasping behavior indicate that, when humans grasp, they intuitively adapt their hand posture according to the object and the task to be executed. Particularly, in [2] grasp selection by humans was studied and post processing of the hand's kinematics verified that humans adopt postures that generally maximize the force/velocity transmission ratios along the directions required for the task to be executed.

The problem of deriving optimal grasps under a detailed task description has been tackled in the past and various methodologies have been proposed, [3]–[6]. Unfortunately, most of the aforementioned approaches suffer from major drawbacks, such as the difficulty in modelling the task ellipsoid, as well as the fact that force closure is not generally guaranteed by the yielded configuration, limiting thus their applicability. As explained in the sequel, it is of great importance in this work not only to balance the task disturbances but also to derive a force closure grasp.

Another issue raised in the majority of analytical approaches on grasping, concerns the assumption that the robot hand fingers can reach the determined contact points accurately and that the object parameters are known precisely. As showed in [7], the existence of many types of uncertainties can even break the force closure property of a grasp; hence they should be taken into account during both grasping posture and contact force selection. Towards this direction, the concept of independent contact regions was introduced to compensate for positioning inaccuracies in grasping; if each contact point is located inside the corresponding regions on the object surface, then force closure is preserved [8], [9], [10].

In this paper, we synthesize a complete framework for deriving a stable robust grasp under certain task specifications. The main novelty of this work consists in the fact that the concept of Q distance, originally proposed by Zhu and Wang [11], is introduced towards incorporating the task specificity in the grasp selection algorithm. In this way, a task oriented optimization problem is formulated that yields an optimal grasp configuration, satisfying simultaneously the kinematic constraints of the robotic hand. Furthermore, based on our previous work on robust grasping [1], a wide range of uncertainties is taken into consideration employing appropriate independent contact regions and sufficient contact forces. Similarly, the contact force transmission ratio of the robotic hand is also maximized. However, in this work our previous approach has been modified in order to deal with the task specifications. Finally, the proposed grasping strategy, is verified by an experimental study on the 15 DoF DLR/HIT II robotic hand attached at the 7 DoF Mitsubishi PA10 robotic manipulator. An appropriate tactile sensor setup was also deployed to minimize the uncertainty level on the contact points and further relax the computation of contact forces.

II. Grasping algorithm

We consider an n_p-fingered robotic hand with n_q rotational joints in total, grasping a rigid object with n_p point-to-point frictional contacts. The hard finger contact model is also adopted, which implies that all force components are transmitted through the contacts. Additionally, according to the friction coulomb model, each of the n_p forces must lie inside its corresponding friction cone in order to avoid slippage. Thus, denoting by μ the friction coefficient, by f_n the normal force component and by f_o, f_t the tangential components, the friction constraints are formulated as:

$$\sqrt{f_{i_o}^2 + f_{i_t}^2} \leq \mu f_{i_n}, \quad i = 1, ..., n_p. \tag{1}$$

Hence, linearizing the friction cone by an n_g-sided polyhedral cone, each grasping force can be represented as:

$$f_i = \sum_{j=1}^{n_g} a_{ij} s_{ij}, \quad a_{ij} \geq 0,$$

with s_{ij} denoting the j^{th} edge vector of the linearized friction cone. Consequently, the wrench produced by f_i is given by:

The authors are with the Control Systems Lab, School of Mechanical Engineering, National Technical University of Athens, 9 Heroon Polytechniou Str, Athens, 15780, Greece. Email: mc08058@mail.ntua.gr, chmpechl@gmail.com, mliaro@mail.ntua.gr, kkyria@mail.ntua.gr

This work has been partially supported by the European Commission with the Integrated Project: THE Hand Embodied, no. 248587 as well as the STREP: RECONFIG: Cognitive, Decentralized Coordination of Heterogeneous Multi-Robot Systems via Reconfigurable Task Planning, no. 600825, within the FP7-ICT calls on Cognitive Systems and Robotics.

$$w_i = \begin{pmatrix} f_i \\ f_i \times p_i \end{pmatrix} = \sum_{j=1}^{n_g} a_{ij} \begin{pmatrix} s_{ij} \\ s_{ij} \times p_i \end{pmatrix}$$

where the vectors $w_{ij} = \begin{pmatrix} s_{ij} \\ s_{ij} \times p_i \end{pmatrix} \in \Re^6$ define the primitive wrenches (i.e., the wrench generated by a force along the j^{th} edge of the linearized friction cone) with p_i denoting the position of i^{th} contact point with respect to the object coordinate frame. Finally, the magnitude of the forces along the n_g edges of the friction cone is considered to be F_G.

In this way, the grasp is force closured if and only if the primitive wrenches positively span the entire wrench space, or equivalently the origin of the wrench space lies strictly inside the convex hull of the primitive wrenches (i.e., $\mathbf{0} \in \text{int}(\mathbf{co}(w_{11}, w_{12}, ..., w_{n_p n_g}))$) [12]. Notice, also, that the convex hull of the primitive wrenches, or else the *Grasp Wrench Space* (*GWS*), includes the set of wrenches that can be exerted on the object when the sum of the forces' magnitudes is bounded by F_G.

A. Task specific grasping posture

The proposed task specific grasp selection algorithm is based on the concept of the Q distance, originally proposed in [11], for curved objects. Given a compact convex set $Q \subset \mathbb{R}^m$ that contains the origin (i.e., $\mathbf{0} \in \text{int}(Q)$) and any point $\mathbf{a} \in \mathbb{R}^m$, the gauge function of Q is defined as:

$$g_Q(\mathbf{a}) = \{\inf \gamma \mid \mathbf{a} \in \gamma Q\}$$

Notice further that $g_Q(\cdot)$ may be considered as a pseudonorm [11]. In addition, the origin centered Q-sphere in terms of g_Q is defined as: $S_Q = \rho Q = \{\mathbf{a} \in \mathbb{R}^m \mid g_Q(\mathbf{a}) \leq \rho\}$, where ρ denotes the radius[1].

The authors in [11] showed that if $Q \subset \mathbb{R}^m$ is restricted to be a polyhedral set, the Q-distance d_Q from p to A, where $p \in \mathbb{R}^m$ is a point and $A \subset \mathbb{R}^m$ a convex polyhedron, is calculated in terms of g_Q as follows:

$-p \notin \text{int}(A)$:	$-p \in \text{int}(A)$:
$d_Q^+(p,A) = \min \sum_{k=1}^{K} \rho_k$ s.t. $\left\{ \sum_{k=1}^{K} \rho_k q_k = \sum_{i=1}^{N} \alpha_i \mathrm{a}_i - p,\ \sum_{i=1}^{N} \alpha_i = 1,\ \rho_k, \alpha_i \geq 0 \right\}$	$d_Q^-(k) = \min(-\rho)$ s.t. $\left\{ \rho q_k = \sum_{i=1}^{N} \alpha_i \mathrm{a}_i - p,\ \sum_{i=1}^{N} \alpha_i = 1,\ \alpha_i, \rho \geq 0 \right\}$ $d_Q^-(p,A) = \max_{k=1,...,K} d_Q^-(k)$

where $q_k,\ k = 1,...,K$ and $\mathrm{a}_i,\ i = 1,...,N$ are the vertices of Q and A respectively. Notice that the aforementioned linear programs can be easily solved using the simplex method.

Assume that W contains the primitive wrenches of the grasp configuration ($m = 6$). As noted in [11], the equality $d_Q^+(\mathbf{0}, \mathbf{co}(W)) = 0$ represents a necessary condition for the force closure property, while the inequality $d_Q^-(\mathbf{0}, \mathbf{co}(W)) < 0$ is equivalent to $\mathbf{0} \in \text{int}(\mathbf{co}(W))$ and can be interpreted as a sufficient condition. Furthermore, the quantity $|d_Q^-(\mathbf{0}, \mathbf{co}(W))|$ is consistent with the popular quality metric defined in [13], except that the euclidean distance is replaced by the Q-distance. Thus, an optimal force closure grasp can be obtained by minimizing:

$$d_Q(\mathbf{0}, \mathbf{co}(W)) = \begin{cases} d_Q^+(\mathbf{0}, \mathbf{co}(W)), & \mathbf{0} \notin \text{int}\ (\mathbf{co}(W)) \\ d_Q^-(\mathbf{0}, \mathbf{co}(W)), & \mathbf{0} \in \text{int}\ (\mathbf{co}(W)) \end{cases}$$

Notice, also, that $-d_Q^-(\mathbf{0}, \mathbf{co}(W))$ can be geometrically interpreted as the largest radius of the Q-sphere contained in $\mathbf{co}(W)$. Therefore, minimizing $d_Q^-(\mathbf{0}, \mathbf{co}(W))$ leads to a grasp configuration that maximizes the radius of the Q sphere inside the convex hull of the primitive wrenches. To proceed, notice that the utilized quality measure is tightly connected to the Q set; thus, the optimal configuration can be adjusted through appropriate modification of Q. To illustrate this point let us consider Fig. 1. In these images two hypothetical convex hulls are depicted, for two grasp configurations. The quality metric used in the first case is the L_2 norm, while in the second case the adopted Q-set differs significantly from the L_2 sphere. It is obvious that the convenient L_2 norm evaluates equally these two cases. In contrast, the Q-distance discriminates the two configurations according to the task specifications imposed by the Q-set.

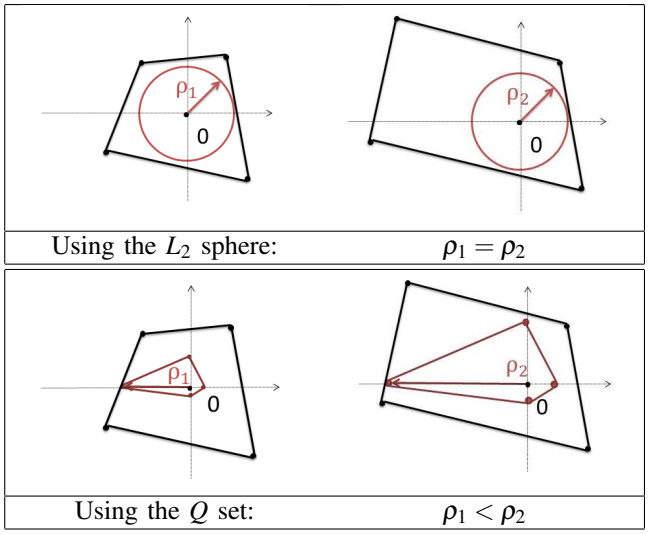

Fig. 1. A hypothetical example illustrating the advantage of the Q distance over the L_2 norm in evaluating the task specificity of grasp configurations.

Considering the above and aiming at formulating a task oriented optimization problem, the Q set should contain the origin as well as those wrenches that need to be applied by the robotic hand in order to balance the task disturbances. Therefore, instead of just guaranteeing the force closure property as in [11], the obtained configuration will be able to compensate disturbances in particular directions with relatively low forces. Finally, it should be mentioned that the sum of the task disturbances' magnitudes, F_t, should be lower or equal than the sum of contact forces ($F_t \leq F_G$) [10].

To calculate task specific grasping postures in the context of Q-distance, we formulate our optimization problem with

[1] In case Q is the L_2 sphere then g_Q is the same as the L_2 norm.

the unified vector $v = \begin{bmatrix} q & w \end{bmatrix}^T$ as decision variable, where $q \in \mathbb{R}^{n_q}$ and $w \in \mathbb{R}^6$ denote the joint displacements and wrist position/orientation respectively. We further assume that the desired position/orientation of the robotic hand can be implemented by attaching it on a dexterous manipulator. Thus, the optimization problem is defined as follows:

$$\min \; d_Q(\mathbf{0}, \mathbf{co}(W))$$

s.t.

$$q_{min} \leq q \leq q_{max} \tag{2}$$
$$fkine(q) \in \partial O \tag{3}$$
$$q^j_{abd/add} \leq q^{j+1}_{abd/add} \tag{4}$$
$$p' \notin O \tag{5}$$

Equation (2) describes the joint mechanical limits whereas (3) ensures that the fingertips are in contact with the object surface. Furthermore, $q^j_{abd/add}, (j = 1, ..., n_p - 1)$ represents the abduction/adduction degree of freedom. Hence, equation (4) prevents collision between consecutive robotic fingers. The last constraint is added in order to avoid penetration between the robotic hand and the object. In particular, p' denotes a set of finite discrete points lying on the robotic hand (the fingertips are excluded). Thus, given an analytical expression of the object boundary, equation (5) can be easily expressed as inequality constraints. Henceforth, we shall refer to these constraints using the abbreviation *RHC*, (*Robotic Hand Constraints*).

B. Dealing with force transmission maximization and positioning inaccuracies

Robotic hands are also subjected to joint torque constraints. Thus, it is important to adopt a robot hand configuration that is capable of exerting the required grasping forces on the object with relatively low joint torque effort. Towards this goal, we exploited the force transmission ratio r_k and compatibility index c which was originally defined in [4] as:

$$r_k = [u_k^T (J_i J_i^T) u_k]^{-1/2}, \; c_i = \sum_{k=1}^{l} r_k^2 = \sum_{k=1}^{l} [u_k^T (J_i J_i^T)^u_k]^{-1}$$

where $u_k, \; k = 1, ..., l$, denotes the direction of interest for the contact forces and J_i denotes the jacobian of the i^{th} finger, $i = 1, ..., n_p$. For each contact point we choose the unit vectors u_k to be aligned with the edges of the linearized friction cone as in [14], thus maximization of: $c = \sum_{i=1}^{n_p} w_{f_i} c_i$, where w_{f_i} are weighting factors, yields an optimal posture with respect to the force transmission metric.

Since deviation between the actual and desired joint positions is inevitable, we must guarantee that the robotic hand can perform the given task despite fingertip positioning inaccuracies. Therefore, we utilized the concept of independent contact regions (*ICR*), adopting, in particular, the approach described in [10] to determine whether a point on the object boundary qualifies to be a member of an *ICR*.

In summary, consider a given force closure grasp configuration that contains the set of task wrenches (*Task Wrench Space*, *TWS*). Each ICR_i consists of a set of discrete points, such that if the fingertips are placed inside the corresponding region, a force closure grasp is obtained that can balance the task disturbances. The procedure of computing the *ICRs* based on the particular method is illustrated in Fig. 2 for a hypothetical 2-d wrench space. A convex hull of 3 contact points is illustrated that contains the *TWS* (red colour). Each contact point p_i is associated with two primitive wrenches w_{ij} and a number of facets F_k, involving at least one vertex w_{ij}.

In our work, the range of the joint displacement error of the robotic hand is known, hence the deviation of the contact points can be computed. Therefore, instead of checking which points on the object boundary qualify to be inside the *ICRs*, as in [9], [10], we check whether the necessary hyperplane displacements H'_k satisfy the task constraints (i.e., the *TWS* belongs in $\bigcap H'^{-}_k$). Thus, given: i) the nominal contact points p_i, ii) the hyperplanes' equations $H_k x = K_k$, iii) the deviated contact points $p_{is}, s = 1, ..., S$ for each p_i as well as iv) the set of task disturbances $t_\delta \in TWS, \delta = 1, ..., \Delta$, we can compute the distance of H'_k from $\mathbf{0}$ when it is built tangent to the *TWS* as $D_k = \max(H_k t_\delta) > 0$. This quantity denotes the minimum required distance between H'_k and $\mathbf{0}$ so that the *TWS* will be contained in the *GWS* . Consequently, whether the deviated contact points belong in their respective *ICR*, can be determined as follows:

for $i \leftarrow 1$ **to** n_p (*ie for each contact point*, p_i) **do**
  for $j \leftarrow 1$ **to** n_g (*ie for each prim wrench*, w_{ij}) **do**
    find hyperplanes H_k that involve w_{ij}
    for $k \leftarrow 1$ **to** K (*ie for each* H_k *of* w_{ij}) **do**
      for $s \leftarrow 1$ **to** S (*ie for each deviated* p_{is}) **do**
        compute the maximum possible distance κ_s=max($H_k w_{i_{sj}}$) of H'_k from $\mathbf{0}$ so that at least one primitive wrench of p_{is} belongs in H'^{+}_k
      end
      compute the required signed distance $\Lambda_k = \min(\kappa_s)$ of H'_k from $\mathbf{0}$ so that at least one primitive wrench of all p_{is} belongs in H'^{+}_k
      if $\Lambda_k < D_k$ **then**
        $p_{is} \notin ICR_i$
        break
      end
    end
  end
  $p_{is} \in ICR_i, s = 1, ..., S$ (ie all uncertainties p_{is} of p_i belong in ICR_i)
end

Notice that, if $\Lambda_k < D_k$ at least one hyperplane H'_k that involves a primitive wrench of the deviated contact points does not contain the *TWS*.

In this work, the *TWS* is represented by the Q set defined in Subsection II-A. Considering the analysis above and keeping as decision variables the unified vector $v = \begin{pmatrix} q & w \end{pmatrix}^T$, we formulate an optimization problem that yields a grasp

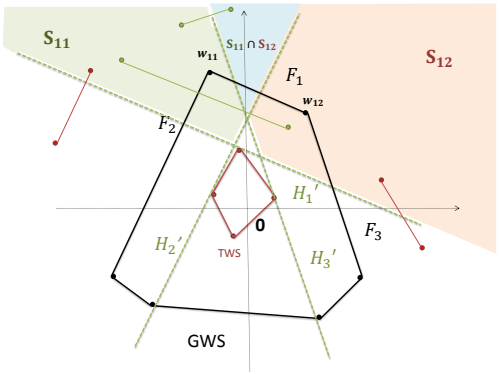

Fig. 2. w_{11} of contact point p_1 is associated with facets F_1 and F_2. H_1', H_2' are the hyperplanes built parallel to F_1, F_2 respectively and tangent to TWS, leaving $\mathbf{0}$ and their corresponding facet at different halfspaces. Assuming that $\mathbf{co}(W) \subseteq H_k^-$, the intersection of the halfspaces $H_1'^+, H_2'^+$ is named S_{11} ($S_{11} = \bigcap H_k'^+, k = 1,2$). S_{12} may be created for w_{12} similarly. A neighboring point is said to be included in the ICR_1 if its primitive wrenches (green colour) lie inside S_{11} and S_{12} respectively.

configuration with optimal force transmission and robustness against positioning inaccuracies as follows:

$$\min \ \frac{1}{c}$$

s.t.

$$RHC$$

$$d_Q^-(\mathbf{0}, \mathbf{co}(W)) < 0 \quad (6)$$

$$p_{is} \in ICR_i \quad (7)$$

Equation (6) enforces the algorithm to search only force closured grasps. Moreover, equation (7) enforces the deviated contact points p_{is} to belong in their corresponding independent contact region. Finally, the initial posture provided to the algorithm is the one calculated in Subsection II-A. As the authors in [9] state, an optimal configuration with respect to the utilized quality metric (defined in [13]) results in larger ICRs. In light of this, the task oriented optimal grasp configuration generated in Subsection II-A is ideal to initiate our second search algorithm.

C. Determining contact forces via tactile sensing

1) Introducing tactile sensing: In our work, we used the off-the-shelf 4256e Grip sensor designed by Tekscan. This ultra thin tactile sensor is able to measure the pressure magnitude of each sensel based on piezo-resistive technology. The active region of each fingertip is a 4x4 array and the sensels' output allows us to compute the center of force, or equivalently, the contact centroid as:

$$x_{cof} = \frac{\sum_{i=0}^{3} x_i \sum_{j=0}^{3} p_{ij}}{\sum_{i=0}^{3}\sum_{j=0}^{3} p_{ij}}, y_{cof} = \frac{\sum_{j=0}^{3} y_j \sum_{i=0}^{3} p_{ij}}{\sum_{j=0}^{3}\sum_{i=0}^{3} p_{ij}}$$

where p_{ij} is the pressure value at each sensel and x_i, y_j denote the x-coordinate of i^{th} column and the y-coordinate of j^{th} row respectively on the 4x4 array.

The position of the contact centroids is defined by 2-D coordinates on the arrays of the tactile sensor. However, it is required to map the centroid local coordinates (x_{cof}, y_{cof}) into 3-D coordinates on the fingertip. Towards this goal, we exploited the point cloud of the robotic fingertips (in our case for the DLR/HIT II robotic hand). For each robotic finger, we, initially, matched the 4 corner sensels of the array with their actual position $p_i^{corn}, i = 1,...,4$, on the point cloud and computed the distance from them to all other nodes of the point cloud. Assuming that the Grip sensor covers firmly the surface of the fingertips owing to its inherent thinness and flexibility, given a contact centroid on each array (x_{cof}, y_{cof}) we determined its corresponding node P(X,Y,Z) on the point cloud of the robotic fingertip by minimizing the function:

$$\min\{ \sum_{i=1}^{4} (dist_i(X,Y,Z) - arraydist_i(x_{cof}, y_{cof}))^2 \} \quad (8)$$

where $dist_i(X,Y,Z)$ denotes the distance from p_i^{corn} to node P(X,Y,Z) on the point cloud and $arraydist_i(x_{cof}, y_{cof})$ denotes the distance between the i^{th} corner sensel and the contact centroid on the tactile array. In other words, we assumed that the distance between two points remains invariant whether they are expressed by 3-D coordinates or 2-D coordinates on the arrays.

2) The grasping strategy: With the aforementioned tactile sensing capabilities, we present the following grasping strategy:

1) Offline search for a task specific robust configuration (i.e., joint angles and wrist position/orientation) as presented in Subsections II-A and II-B.
2) Implementation of the desired configuration.
3) Stop robotic finger motion when contact with the object has been detected by the corresponding tactile sensor.
4) Obtain the actual joint positions and contact centroids from the encoders and the tactile sensors respectively.
5) Map the contact centroids to their corresponding position on the mechanical fingertips using (8) as presented is Subsecion II-C.
6) Compute the position of the contact points on the object through forward kinematics.
7) Determine sufficient forces to grasp the object.

It should be noticed that the measuring errors of the joint angle sensors are considered to be negligible. Hence, any errors in the contact points computation in Step 6, may appear only owing to uncertainties in the centroids' measurements.

In the sequel, we present the algorithm that calculates online adequate contact forces to ensure object immobility. The expressions that relate the contact forces f_c with the external disturbance w_{ext} and the joint torques τ are:

$$G f_c = -w_{ext} \quad (9)$$

$$J^T f_c = \tau \quad (10)$$

where G and J denote the grasp matrix and jacobian respectively ($J = diag(J_i), i = 1,...,n_p$) [15]. Furthermore, from (9) the contact forces can be written as:

$$f_c = -G^+ w_{ext} + E\lambda, \quad (11)$$

where G^+ is the pseudoinverse of G, E is a matrix whose columns form a basis for the nullspace of G and λ is an arbitrary vector. The first term of (11) is related to the

compensation of external wrench w_{ext}, while the term $E\lambda$ denotes those forces whose resultant wrench to the object is null [15]. The set of these forces is known as internal forces. By exerting internal forces on the object appropriately, the generated contact forces comply with the friction constraints. Thus, our goal in this section is to calculate and apply appropriate internal forces to the object so that the friction law and torque constraints are not violated.

Assume that the maximum absolute value of the uncertainty on the fingertips is δp_{max}. In our approach the magnitude of the uncertainty on the object geometry will also be considered as δp_{max}. To proceed, the authors in [16] proposed that even if contact uncertainties occur, equation (9) needs to be satisfied in order to grasp the object successfully. Thus, by representing as δx the deviation of x due to δp and neglecting higher order terms, equation (9) becomes:

$$-w_{ext} = Gf_c = (\delta G + G)(\delta f_c + f_c)$$
$$\Rightarrow \delta f_c = -G^{+}\delta G f_c \quad (12)$$

After straightforward matrix norm calculations and utilizing the ortho-normality of the rotation matrices, (12) lead in:

$$\|\delta f_{c_i}\| \leq \|\delta f_{c_{i_{max}}}\| = \|\Xi_i G^{+} \begin{bmatrix} 0 \\ I_{3x3} \end{bmatrix}\| \delta p_{max} \sqrt{1+\mu^2} \sum_{i=1}^{n_p} f_{n_i} \quad (13)$$

where Ξ_i represents a separation matrix $(f_{c_i} = \Xi_i f_c)$, $f_{n_i} = n_i f_{c_i}$ is the normal force component and n_i is the contact normal vector. Similarly, from equation (10) we get for the k^{th} joint:

$$\delta\tau_{i_k} = \delta J_{i_k}^T f_{c_i} + J_{i_k}^T \delta f_{c_i} \quad (14)$$

In our case, as explained in Subsection IIC 2), joint displacement errors are negligible, hence $(\partial J_{i_k}/\partial q_{i_k})\delta q_{i_k} = 0$. Consequently, it can be shown for the k^{th} joint that:

$$|\delta\tau_{i_k}| \leq |\delta\tau_{i_{kmax}}| = \sqrt{1+\mu^2}\delta p_{max} f_{n_i} + \|J_{i_k}\|^T \|\delta f_{c_{i_{max}}}\| \quad (15)$$

It should be noted that contact uncertainty affects the friction cone as well. In light of this, a new friction coefficient for curved objects can be determined as [16]:

$$\theta_{max} = 2sin^{-1}\frac{\delta p_{max}}{2r}, \quad r: curvature\ radius$$
$$\mu' = tan(tan^{-1}\mu - \theta_{max})$$

In order to take into consideration the contact forces and joint torques deviation, the authors in [16] proposed to increase the normal force component in the friction law by $\|\delta f_{c_{max}}\|$ (13) and reduce the maximum actuator torque by $|\delta\tau_{i_{kmax}}|$ (15). Moreover, the friction cone defined in (1) may be approximated by an L-sided convex polyhedral cone in order to reduce the computational complexity of the problem [17]. Hence, (1) can be expressed as: $-V_i f_{c_i} \leq \mathbf{0}, \quad f_{n_i} \geq 0$.

Considering as decision variables the vector λ of the internal forces defined in (11), the linear optimization problem towards determining sufficient internal forces is formulated:

$$\min \sum f_{n_i}$$

s.t.

$$-V_i'(f_{c_i} - n_i\|f_{c_{i_{max}}}\|) \leq \mathbf{0}$$
$$|\tau_{i_k}| \leq |\tau_{i_{k_{max}}}| - |\delta\tau_{i_{k_{max}}}|$$
$$f_{n_i} \geq 0$$

$i = 1,...,n_p, k = 1,...,K$, where in V' the friction coefficient μ' is used instead of μ. The algorithm presented above searches for internal forces that minimize the sum of the normal forces and therefore the grasp effort, while simultaneously constraining the generated contact forces to satisfy the friction and torque constraints. The contact forces and joint torques produced by the internal forces are computed in the optimization scheme through equations (10), (11).

Remark 1: In contrary with [16], the tactile sensors allows us to neglect joint angle errors and take into account only potential errors on the fingertips. Furthermore, in our analysis, the posture of the robotic hand is determined by maximizing the force transmission ratio, as presented in Subsection II-B, whereas by exploiting tactile sensing we further reduce the range of uncertainty regarding the grasping parameters, thus relaxing significantly the on-line calculation of the internal forces. Apparently, in this way the two parts of the proposed grasping strategy (i.e., the off-line and the on-line) are tightly interconnected towards generating successful grasps.

III. Experimental results and validation

A. Task description

Our experimental procedure considers the stable grasp of a cylindrical object filled with liquid, while it is being rotated about one axis. Four different states of the object are depicted in Fig. 3, all of which are used to model our task disturbances. More specifically, the rotation is implemented about the z axis, while it is assumed that the liquid is distributed symmetrically about the particular axis. In these images the black dot denotes the center of mass for each state of the object, while the object coordinate frame is determined by the red axis. Thus, it can be inferred that the object's weight at the depicted states causes external forces along the x and y axis, as well as external moments about the z axis of the object coordinate frame.

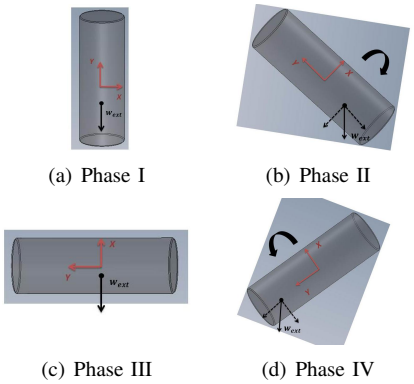

(a) Phase I (b) Phase II

(c) Phase III (d) Phase IV

Fig. 3. Task description

B. Output of the algorithms for the task specifications

The object to be grasped was considered to be a 2.25 cm-radius, 13 cm-high cylinder. Given the task and object characteristics, the algorithms in Subsections II-A, II-B yielded off-line an optimal posture illustrated in Fig. 4. For the derived configuration we considered an 8-sided

linearized friction cone and, due to the robust nature of our analysis, we selected a conservative friction coefficient [7] ($\mu = 0.3$). Furthermore based on the joint displacement error of the DLR/HIT II robotic hand, the maximum contact point deviation on the object was found to be 4 mm. Hence, for the computation of the *ICRs* presented in Subsection II-B, four deviated contact points (denoted as p_{is}) were considered at a distance of 4 mm from their corresponding nominal contact point. It should be mentioned that, the influence of uncertainties related to the friction coefficient and object model were considered for the *ICRs* determination as presented in [18]. The solution of the optimization schemes was derived using the MATLAB Optimization Toolbox.

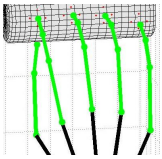

Fig. 4. Optimal configuration (red dots denote the contact points uncertainties)

In order to perform the given task the required internal forces are computed by solving the algorithm presented in Subsection II-C. In our work w_{ext} in (11) is considered to be the set of task disturbances that appear throughout the experimental procedure (see Fig. 3). The uncertainty of the center of mass location, can be represented as a set of external wrenches with respect to the nominal position of the center of mass. Consequently, instead of compensating the nominal task disturbances $w_t, t = 1,...,T$, we search for internal forces that compensate a set w_{tl}, $l = 1,...,L$, of external disturbances, where w_{tl} denotes the l center of mass uncertainty for the t task disturbance. In other words, the derived internal forces should produce, for each external wrench w_{tl}, contact forces (11) that satisfy the friction and torque constraints. In this respect, note also that the Q set determined in Subsection II-A should not only include the nominal task loads, but also the external wrenches associated with the uncertainty in the center of mass.

In Fig. 5 we present the desired angles q and torques τ. The uncertainty of the contact points δp_{max} and the center of mass is considered to be 1 and 3 cm respectively.

C. Experimental validation

The DLR/HIT II robotic hand is attached at the end effector of the Mitsubishi PA10 manipulator and the tactile arrays are mounted on the robotic fingertips. Note, also, that due to the high accuracy we have in terms of positioning the Mitsubishi PA10 end effector, we neglect errors in the actual wrist position/orientation.

In order to exert the desired forces the the necessary motor displacements were calculated via the dynamic model as in [1]. In the attached video the grasping procedure is illustrated in order to validate the proposed methodology. The video can be found also in HD quality in the following URL: https://www.youtube.com/watch?v=lkpSgamV0b8.

Thumb	q	τ	**Index**	q	τ
a/a	-12.4	0.12	a/a	-9.1	-0.07
f/e 1	8.9	0.34	f/e 1	22.8	0.13
f/e 2	10.9	0.17	f/e 2	13	0.07
Middle	q	τ	**Ring**	q	τ
a/a	-4.3	-0.01	a/a	0.3	0
f/e 1	12	0.07	f/e 1	10.8	0.09
f/e 2	35.2	0.04	f/ext 2	33.2	0.07

Pinky	q	τ
a/a	5.2	0
f/e 1	12.5	0.03
f/e 2	21	0.01

Fig. 5. Experimental data (q :degrees, τ : Nm, "a/a": abduction/adduction DoF,"f/e": flexion/extension DoF)

REFERENCES

[1] G. I. Boutselis, C. P. Bechlioulis, M. V. Liarokapis, and K. J. Kyriakopoulos., "An integrated approach towards robust grasping with tactile sensing," *Robotics and Automation, Proceedings. IEEE International Conference on*, 2014.

[2] J. Friedman and T. Flash, "Task-dependent selection of grasp kinematics and stiffness in human object manipulation," *Cortex*, 2007.

[3] M. Teichmann and B. Mishra, "Probabilistic algorithms for efficient grasping and fixturing," *Algorithmica*, 2000.

[4] S. L. Chiu, "Task compatibility of manipulator postures." *I. J. Robotic Res.*, vol. 7, no. 5, pp. 13–21, 1988.

[5] Z. Li and S. Sastry, "Task-oriented optimal grasping by multifingered robotic hands," *IEEE J. Robotics and Automation*, 1988.

[6] C. I. Mavrogiannis, C. P. Bechlioulis, M. V. Liarokapis, and K. J. Kyriakopoulos, "Task-specific grasp selection for underactuated hands," *Robotics and Automation, Proceedings. IEEE International Conference on*, 2014.

[7] Y. Zheng and W.-H. Qian, "Coping with the grasping uncertainties in force-closure analysis." *I. J. Robotic Res.*, vol. 24, no. 4, pp. 311–327, 2005.

[8] J. Ponce, S. Sullivan, A. Sudsang, J.-D. Boissonnat, and J.-P. Merlet, "On computing four-finger equilibrium and force-closure grasps of polyhedral objects." *I. J. Robotic Res.*, vol. 16, no. 1, pp. 11–35, 1997.

[9] M. Roa and R. Suarez, "Computation of independent contact regions for grasping 3-d objects," *Robotics, IEEE Transactions on*, vol. 25, no. 4, pp. 839–850, 2009.

[10] R. Krug, D. Dimitrov, K. Charusta, and B. Iliev, "On the efficient computation of independent contact regions for force closure grasps," in *Intelligent Robots and Systems (IROS), 2010 IEEE/RSJ International Conference on*, 2010, pp. 586–591.

[11] X. Zhu and J. Wang, "Synthesis of force-closure grasps on 3-d objects based on the q distance," *Robotics and Automation, IEEE Transactions on*, vol. 19, no. 4, pp. 669–679, 2003.

[12] R. M. Murray, S. S. Sastry, and L. Zexiang, *A Mathematical Introduction to Robotic Manipulation*, 1st ed. Boca Raton, FL, USA: CRC Press, Inc., 1994.

[13] D. G. Kirkpatrick, B. Mishra, and C.-K. Yap, "Quantitative steinitz's theorems with applications to multifingered grasping." ACM, 1990, pp. 341–351.

[14] R. D. Hester, M. Cetin, C. Kapoor, and D. Tesar, "A criteria-based approach to grasp synthesis," in *Robotics and Automation, 1999. Proceedings. 1999 IEEE International Conference on*, vol. 2, 1999, pp. 1255–1260 vol.2.

[15] B. Siciliano and O. Khatib, Eds., *Springer Handbook of Robotics*. Springer, 2008.

[16] P. Fungtammasan and T. Watanabe, "Grasp input optimization taking contact position and object information uncertainties into consideration," *Robotics, IEEE Transactions on*, vol. 28, no. 5, pp. 1170–1177, 2012.

[17] J. Kerr and B. Roth, "Analysis of multifingered hands," *Research, The International Journal of Robotics*, 1986.

[18] M. Roa and R. Suarez, "Influence of contact types and uncertainties in the computation of independent contact regions," in *Robotics and Automation (ICRA), 2011 IEEE International Conference on*, 2011, pp. 3317–3323.